Research Article

Bojana Aleksova*, Ivica Milevski, Risto Mijalov, Slobodan B. Marković, Vladimir M. Cvetković, and Tin Lukić

Assessing risk-prone areas in the Kratovska Reka catchment (North Macedonia) by integrating advanced geospatial analytics and flash flood potential index

https://doi.org/10.1515/geo-2022-0684
received March 27, 2024; accepted July 08, 2024

Abstract: This study presents a comprehensive analysis of flash flood susceptibility in the Kratovska Reka catchment area of Northeastern North Macedonia, integrating Geographic Information System, remote sensing, and field survey data. Key factors influencing flash flood dynamics, including Slope, Lithology, Land use, and Vegetation index, were investigated to develop the Flash Flood Potential Index (FFPI). Mapping slope variation using a 5-m Digital Elevation Model (DEM) revealed higher slopes in eastern tributaries compared to western counterparts. Lithological units were classified based on susceptibility to erosion processes, with clastic sediments identified as most prone to flash floods. Land use analysis highlighted non-irrigated agricultural surfaces and areas with sparse vegetation as highly susceptible. Integration of these factors into the FFPI model provided insights into flash flood susceptibility, with results indicating a medium risk across the catchment. The average value of the FFPI is 1.9, considering that the values range from 1 to 5. Also, terrains susceptible to flash floods were found to be 49.34%, classified as medium risk. Field survey data validated the model, revealing a significant overlap between hotspot areas for flash floods and high-risk regions identified by the FFPI. An average FFPI coefficient was calculated for each tributary (sub-catchment) of the Kratovska Reka. According to the model, Latišnica had the highest average coefficient of susceptibility to potential flash floods, with a value of 2.16. These findings offer valuable insights for spatial planning and flood risk management, with implications for both local and national-scale applications. Future research directions include incorporating machine learning techniques to enhance modeling accuracy and reduce subjectivity in assigning weighting factors.

Keywords: FFPI, flash floods risk, Kratovska Reka, GIS, geospatial analytics, Remote Sensing, natural hazards

1 Introduction

As mentioned in the study [1], South-Eastern Europe (SEE) has emerged as a global hotspot due to the increasing occurrence of weather-related hazards. Recent studies underscore Europe's vulnerability to hydro-meteorological hazards, particularly flash floods, which pose significant risks to environmental stability, population centers, infrastructure, and socio-economic facets [2–5]. In the SEE region, heavy precipitation-induced flash floods constitute a major hazard [6,7]. Given their unpredictable nature and potential for catastrophic consequences, there is an urgent need to prioritize enhancing early warning systems [8]. Strengthening these systems empowers societies to manage flash flood threats effectively, enabling timely interventions to safeguard vulnerable populations [4].

Flash floods are among the most devastating natural hazards affecting North Macedonia, where various methods,

*** Corresponding author: Bojana Aleksova**, Maarif International School – Skopje Campus, Kiro Gligorov 5, 1000, Skopje, North Macedonia, e-mail: bojana.aleksova@mk.maarifschools.org
Ivica Milevski, Risto Mijalov: Institute of Geography, Faculty of Natural Sciences and Mathematics, Ss. Cyril and Methodius University, Arhimedova 3, 1000, Skopje, North Macedonia
Slobodan B. Marković: Department of Geography, Tourism and Hotel Management, Faculty of Sciences, University of Novi Sad, Trg Dositeja Obradovića 3, 21000, Novi Sad, Serbia; Serbian Academy of Sciences and Arts, Kneza Mihaila 35, 11000, Belgrade, Serbia
Vladimir M. Cvetković: Faculty of Security Studies, University of Belgrade, Gospodara Vucica 50, 11040, Belgrade, Serbia; Scientific - Professional Society for Disaster Risk Management, Dimitrija Tucovića 121, 11040, Belgrade, Serbia; International Institute for Disaster Research, Dimitrija Tucovića 121, 11040, Belgrade, Serbia
Tin Lukić: Department of Geography, Tourism and Hotel Management, Faculty of Sciences, University of Novi Sad, Trg Dositeja Obradovića 3, 21000, Novi Sad, Serbia

including the Flash Flood Potential Index (FFPI), are used for modeling flash floods in catchment areas [9–13]. Flash floods are characterized by sudden, intense water volumes and sediment transport in torrents [14–17]. Predicting flash floods is challenging, but early signs such as heavy rain, thunderstorms, and rapid snowmelt are critical [18]. These events are influenced by factors such as intense rainfall, soil and basin characteristics, and human activities, exacerbated by climate change and land-use changes [19]. Improved indices like FFPI enhance flash flood warning accuracy [20], supported by Geographic Information System (GIS) for integrated hazard susceptibility mapping [21]. Hydrological responses vary based on physical geography, with deforestation impacting water propagation on slopes [22].

Additional FFPI studies have been conducted [22–34]. North Macedonia faces multiple natural hazards, including geohazards like erosion, landslides, and earthquakes [35–39]. Historically considered natural, these disasters are increasingly influenced by human activities. European flash flood events are extensively studied through international projects like HYDRATE, IFRAMM, and EFFS [27].

With the support of open-source software QGIS 3.34.2 and SAGA GIS 9.3.0, we collected satellite images and developed a comprehensive database for this study. Our primary objective is to assess flood risk areas using a statistical GIS-based approach. Beyond mapping hazards, it is crucial to underscore the importance of preventive measures and evacuation protocols to mitigate and ideally prevent the impacts of such hazards. This study employs an integrated approach combining GIS techniques with the FFPI. Our methodology focuses on identifying flash flood drivers, pinpointing high-risk areas, categorizing flood risk levels, and validating these assessments using historical data and remote sensing inputs in the Kratovska Reka catchment (North Macedonia). This initiative represents an essential first step towards implementing effective mitigation strategies for sustainable management of flash flood risks across local and national levels in North Macedonia.

2 Data and methods

2.1 Overview of the study area

According to the research, the main water artery in the Kratovska Reka catchment (68.5 km^2) with a total of 20 tributaries, i.e., sub-catchments, is located in the NE part of North Macedonia (Figure 1). The tributaries of Kratovska Reka are characterized by their usually branched catchments, formed by several sources. Most of them are mountainous, rapid with gorge valleys, and have a typical V

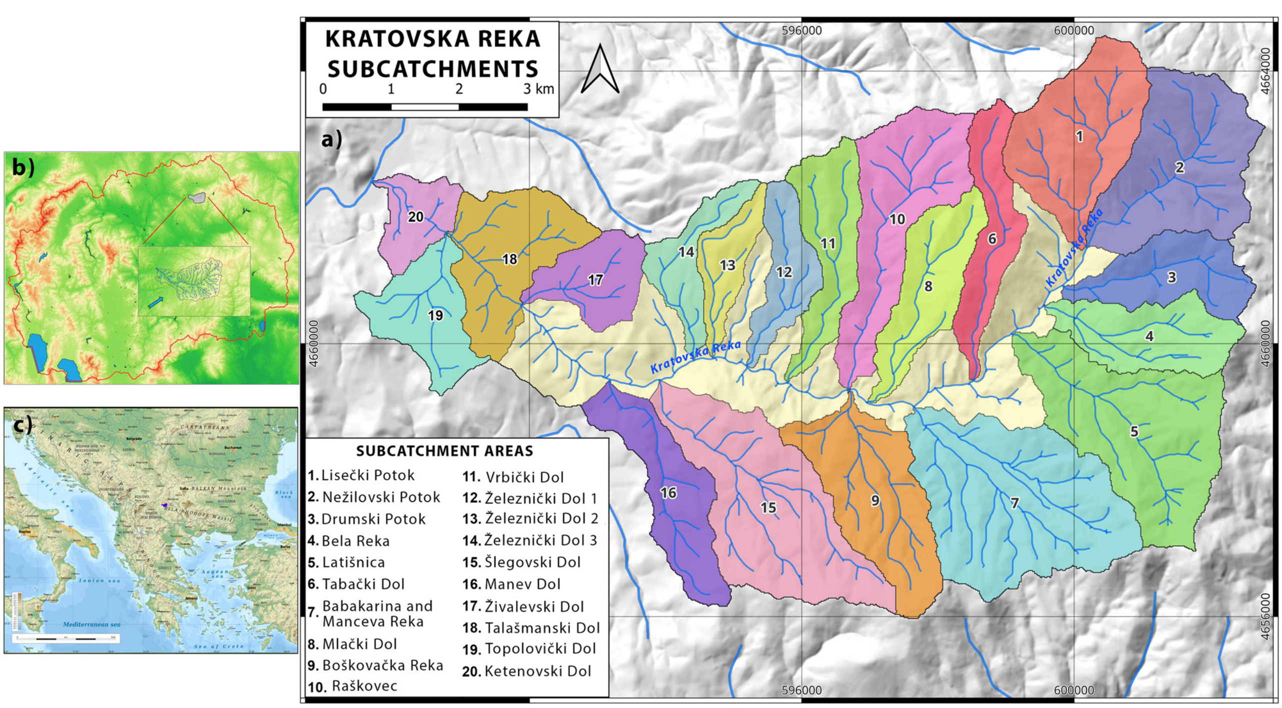

Figure 1: (a) Sub-catchments of Kratovska Reka, (b) Kratovska Reka catchment in the North Macedonia territory, and (c) Kratovska Reka catchment location in the Balkan peninsula (South-East Europe).

profile in the upper course. Throughout most of the year, these tributaries have a large flow of water, which reduces during the summer period [7]. For this work, a digitization and analysis of the sub-basins of the main watercourse Kratovska Reka was carried out. Tables 1 and 2 show the basic hydrographic features of the Kratovska Reka and its more significant tributaries.

Following the performed analyses, it can be observed that Kratovska Reka has 9 left and 8 right tributaries. By area, the largest Sub-catchments are Babakarina and Manceva Reka (6.4 km^2), while the smallest are Ketenovski and Železnički Dol (1.2 km^2). The Ketenovski Dol sub-catchment has the largest coefficient of asymmetry (3.9), while the Talašmanski Dol Sub-catchment has the lowest (1). The Sub-catchment of Lisečki Potok has the highest mean altitude (1194.7 m), whereas the Ketenovski Dol Sub-catchment has the lowest (472.8 m). According to the calculations of the length of the watersheds of the Kratovska Reka catchment, the sub-catchment of Šlegovski Dol has the largest length (12.1 km), and Ketenovski Dol has the shortest length (5.2 km). Additionally, the sub-catchment of Šlegovski Dol has the longest basin length per watercourse (5.2 km), while Ketenovski Dol has the smallest (1.6 km). The results are slightly different regarding azimuth. The sub-catchment of Bela Reka has the highest azimuth value (236.5°), and Topolovički Dol has the lowest value (166.7°). The results also show that the eastern (higher) part of the Kratovska Reka catchment receives the highest precipitation, while the western (lower) part receives the least. According to our calculations, the largest average amount of precipitation is in the sub-catchment of the Nežilovski Potok (801 mm), while the smallest is in the sub-catchment of the Ketenovski Dol (665.2 mm).

Kratovska Reka has a developed hydrographic network. According to our analysis and measurements (based on topographic map (TM) 100k scale and 5-m DEM), the river network consists of 207 permanent, periodic, and occasional watercourses with a total length of 139.6 km. Of these, 30 watercourses (14.5%) are up to 2 km long (total length, 11.8 km), and 177 watercourses (85.5%) are 2–5 km long (total length, 127.8 km).

Among the listed 177 watercourses, 20 are direct tributaries of the Kratovska Reka. These include Nežilovski Potok, Drumski Potok, Bela Reka, Latišnica, Babakarina and Manceva Reka, Boškovačka Reka, Šlegovski Dol, Manev Dol, and Topolovički Dol as left tributaries, and Tabački Dol, Mlački Dol, Raškovec (Figure 2), Vrbički Dol, Železnički 1, 2, and 3 Potok, and Živalevski Dol as right tributaries. Among these, the longest watercourse is Šlegovski Dol (left tributary) with a length of 4.8 km. This indicates that these are relatively short watercourses, with an average length of only 3.1 km.

Table 1: Basic characteristics of the river network of Kratovska Reka and its most important tributaries

Nu.	Sub-catchment	*T*	*P* km^2	AC	H-a m	Lw km	Lc km	a°av	H mm
1.	Lisečki Potok	/	3.8	2.5	1194.7	8.5	3.4	171.4	800.9
2.	Nežilovski Potok	L	4.5	1.3	1179.1	9.8	3.5	212.5	801.0
3.	Drumski Potok	L	2.1	1.3	1131.4	8.0	3.0	235.6	789.3
4.	Bela Reka	L	2.3	1.5	1046.9	7.9	3.2	236.5	773.7
5.	Latišnica	L	5.3	1.5	1077.5	11.9	4.4	196.9	774.6
6.	Tabački Dol	R	2.0	1.1	1068.6	9.7	4.4	183.8	776.3
7.	Babakarina and Manceva Reka	L	6.4	2.0	941.8	11.7	4.2	195.9	748.1
8.	Mlački Dol	R	2.3	1.1	900.3	8.4	3.9	204.3	747.8
9.	Boškovačka Reka	L	3.7	1.5	856.4	9.8	3.8	196.2	732.4
10.	Raškovec	R	3.8	1.2	964.9	11.4	4.8	197.2	759.9
11.	Vrbički Potok	R	2.2	1.7	909.6	9.1	3.9	186.6	748.9
12.	Železnički Dol 1	R	1.5	1.6	819	6.9	2.9	194.9	732.7
13.	Železnički Dol 2	R	1.2	2.4	785.6	6.0	3.1	205.7	725.9
14.	Železnički Dol 3	R	1.4	1.3	739.7	7.5	3.5	205.9	719.0
15.	Šlegovski Dol	L	5.5	1.8	829.9	12.1	5.2	190.2	725.6
16.	Manev Dol	L	2.6	1.4	699.9	9.3	4.1	202.9	701.9
17.	Živalevski Dol	R	1.6	1.4	604.5	5.9	2.0	233.0	691.4
18.	Talašmanski Dol	/	3.0	1.0	548.4	8.7	2.4	195.8	680.4
19.	Topolovički Dol	L	2.0	1.3	577.2	7.6	2.5	166.7	681.4
20.	Ketenovski Dol	/	1.2	3.9	472.8	5.2	1.6	171.6	665.2
	Kratovska Reka	**/**	**68.5**	**1.52**	**881**	**44.7**	**16.9**	**195.8**	**740.6**

T = side of the tributary, *P* km^2 = area, AC = coefficient of asymmetry of the watershed, H-a m = mean height of the catchment, Lw km = watershed length of the catchment, Lc km = maximum catchment length (per watercourse), a°av = mean value of azimuth, H mm = mean amount of precipitation (according to WorldClim 2 data [40].

Table 2: Basic characteristics of the river network of Kratovska Reka and its most important tributaries

Nu.	Sub-catchment	*L* km	Hs m	Hvl m	Δ*m*	Δ‰	Σ*N*	Σ*L* km	*D*
1.	Lisečki Potok	2.9	1338.4	803.4	535.0	184.5	11	7.9	2.1
2.	Nežilovski Potok	3.2	1325.8	803.4	522.4	163.3	20	9.7	2.2
.3.	Drumski Potok	2.9	1279.5	760.5	519.0	179.0	8	4.6	2.2
4.	Bela Reka	2.6	1240.4	738.9	501.5	192.9	9	6.4	2.8
5.	Latišnica	3.8	1203.5	702.7	500.8	131.8	20	11.4	2.2
6.	Tabački Dol	4.1	1251.1	640.0	611.1	149.0	2	4.3	2.2
7.	Babakarina and Manceva Reka	3.6	1145.6	601.8	543.8	151.1	28	18.3	2.9
8.	Mlački Dol	3.6	1049.2	583.8	465.4	129.3	6	5.7	2.5
9.	Boškovačka Reka	3.3	1149.6	573.2	576.4	174.7	12	9.8	2.6
10.	Raškovec	4.4	1136.9	573.2	563.7	128.1	11	8.2	2.2
11.	Vrbički Dol	3.6	1079.2	551.7	527.5	146.5	4	5.1	2.3
12.	Železnički Dol 1	2.7	985.7	532.6	453.1	167.8	4	3.7	2.5
13.	Železnički Dol 2	2.6	954.4	521.8	432.6	166.4	3	4.1	3.4
14.	Železnički Dol 3	3.1	950.4	515.4	435.0	140.3	4	4.1	2.9
15.	Šlegovski Dol	4.8	1075.4	504.7	570.7	118.9	19	13.5	2.5
16.	Manev Dol	3.9	923.6	489.0	434.6	111.4	8	5.9	2.3
17.	Živalevski Dol	1.7	607.7	457.5	150.2	88.4	7	4.0	2.5
18.	Talašmanski Dol	1.5	627.7	443.8	183.9	122.6	17	6.1	2.0
19.	Topolovički Dol	2.2	596.1	432.3	163.8	74.5	8	5.1	2.6
20.	Ketenovski Dol	0.8	482.3	417.2	65.1	81.4	6	1.7	1.4
	Kratovska Reka	**16.9**	**1338.4**	**411.9**	**926.5**	**54.8**	**207**	**139.6**	**2.0**

L, length of the watercourse in km; Hs, height of the source of the watercourse in m; Hvl, elevation of the mouth of the watercourse in m; Δ*m*, total fall of the watercourse in m; Δ‰, average drop of the watercourse in ‰; Σ*N*, total number of watercourses-tributaries; Σ*L*, total length of all tributaries in km; *D*, density of river network in km/km^2.

Figure 2: Raškovec watercourse cut into tuffs, with excessive erosion. Photo: Aleksova B. 2023.

The density of the river network of Kratovska Reka is relatively uniform and amounts to 2.0 km/km^2. According to the data obtained, within the sub-basin areas, it is somewhat higher in the western and southeastern parts of the catchment, specifically in the sub-basins of Železnički Potok 2, Babakarina and Manceva Reka, Železnički Potok 3, Bela Reka, Boškovačka Reka, and Topolovički Potok (3.4–2.6 km/km^2). It should be noted that the eastern part of the watershed, particularly the tributaries of the Kratovska Reka that descend from the Osogovo Mountains (Lisec, 1,526 m), is characterized by a higher mean altitude and greater precipitation. Therefore, their watercourses usually have water throughout the year, with maximum flows during the spring (May and June) and autumn periods (November). These include the sub-basins of Lisečki, Drumski, Nežilovski Potok, Bela Reka, Latišnica (Figure 3), and Tabački Dol (1046.9–1194.7 m).

In general, the left tributaries descend from areas composed of volcanic rocks (andesites, dacites, tuffs, and breccias), while the right tributaries descend from the northwestern part of the Osogovo Mountain Massif (Figure 4). These tributaries have a lower average height (604.5–1068.6 m) with an average height above sea level of 960.9 m and a lower average annual amount of precipitation. Consequently, they have a variable flow and usually dry up during the summer period.

2.2 FFPI method

The FFPI is a statistical method used to identify areas susceptible to flash flooding, commonly applied in both global and regional frameworks [29,41,42]. This method provides a quantitative analysis of areas prone to flash floods based on weighting factors such as slope, vegetation cover, land use, and soil type. Given the scale of the available Soil Map of Macedonia (200k scale), which lacks detailed soil data, the lithological type of the researched area was considered instead. Flash floods in catchment areas are common when soil infiltration rates are reduced due to bare, deforested, and/or steep terrain. Factors like intensive precipitation (combined with snowmelt) [43], terrain slopes, soils, and vegetation density (forest, shrubs, and grasses) contribute to flash flood potential, with less vegetated terrain having a greater risk [44,45].

The FFPI, a widely used method, was first applied at the Colorado River Basin Forecast Center and is based on the US National Weather Service model [46,47]. It is determined using GIS software tools through a statistical approach that correlates various factors with the spatial distribution of watershed drainage [41,42,48–53]. Model values range from 1 to 10 (1 = lowest potential and 10 = highest potential). This model is preferred due to the limitations of meteorological parameters in predicting floods and the lack of a defined connection between this natural hazard and specific physical geographical characteristics.

The structure and texture of soils are key in defining water retention and infiltration. Terrain slopes influence runoff rate and concentration. Vegetation, which affects the retention of atmospheric water on the surface, varies seasonally (e.g., deciduous forests) and can be impacted by wildfires, which reduce soil infiltration due to burned

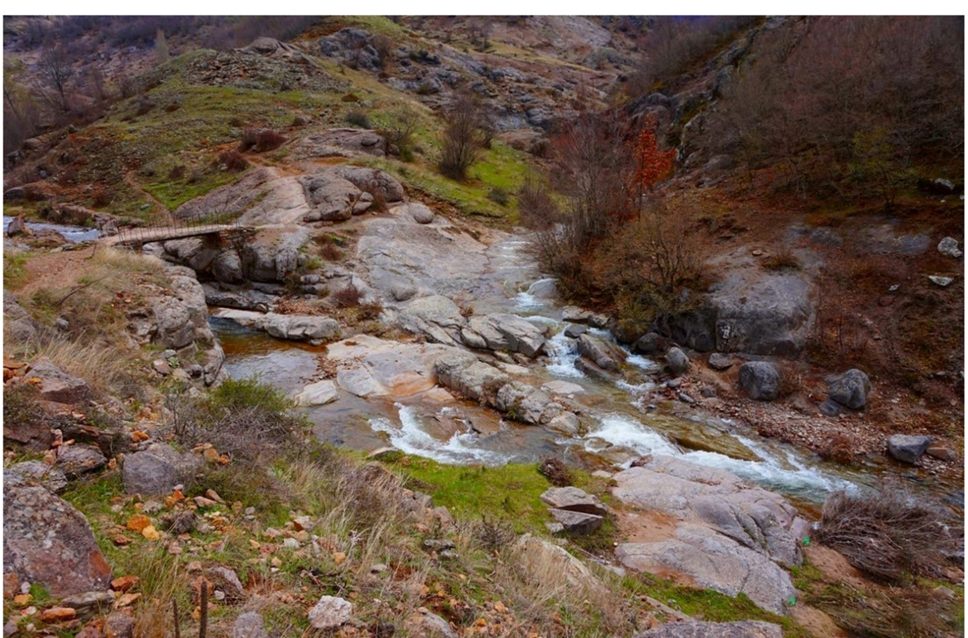

Figure 3: Estuary of Latišnica in Kratovska Reka. Photo: Aleksova B. 2023.

Figure 4: Meander of Kratovska Reka in the upstream part of the catchment. Photo: Aleksova B. 2023.

organic matter. Land use, particularly urbanization, significantly impacts water infiltration, concentration, and outflow from the watershed. These natural conditions collectively provide information on the flash flood potential of a given area [46].

2.3 Data collection for FFPI

To identify flash floods in the Kratovska Reka catchment, an analysis of terrain susceptible to flash floods was conducted using GIS. The FFPI method was used for this analysis. According to the available Soil Map of Macedonia (200k scale), which lacks detailed soil data, the lithological type of the researched area was considered instead of soil types. The following weighting factors were used in developing the model: slope, vegetation cover, lithology, and land use. The FFPI is derived from the formula [47]:

$$\text{FFPI} = (M + S + L + V)/4$$

where M represents the slope of the terrain, S – lithology, L – land use, and V – vegetation index.

The terrain slope (M) was obtained using QGIS 3.32.2-Lima and SAGA GIS 9.0.0 software packages, based on a 15-m DEM (Digital Elevation Model) derived from a 5-m DEM provided by the Ministry for Agriculture, Forestry, and Water Management of North Macedonia. The slope, expressed in percent, is calculated using the formula:

$$M = 10n/30$$

where n represents the average slope of the terrain expressed in %. If n is equal to or greater than 30%, then the M value is always 10. In this case, the average slope (n) in the catchment area of Kratovska Reka is 39.3%. Therefore, M (the slope of the terrain) has a value of 10.

The lithology (S) was analyzed using a digital lithological map based on the Geological Map of Macedonia (100k scale) [54]. Rocks were classified with values from 1 to 9, depending on their susceptibility to erosion.

The land use index (L) was calculated using data from the Corine Land Cover database (2018) [55], with classes assigned values from 1 to 10 based on their impact on flash flooding.

The vegetation index (V) was determined using the Bare Soil Index (BSI) from multispectral satellite imagery obtained through the Landsat 8 program via Earth Explorer, United States Geological Survey [56]. Remote sensing, particularly using the BSI, provides an efficient means to calculate erosion rates correlated with flash floods [57]. The BSI was calculated using the formula [58]:

$$\text{BSI} = [(\text{B6} + \text{B4}) - (\text{B5} + \text{B2})/(\text{B6} + \text{B4}) + (\text{B5} + \text{B2})]$$

where B6 (band 6) represents the short infrared spectral channel (SWIR 1), B4 (band 4) is the red spectral channel, B5 (band 5) is the near-infrared spectral channel (NIR), and B2 (band 2) is the blue spectral channel. After the bands were selected, the images were processed using the Atmospheric correction tool, and then, they were cut in the domain of the watershed boundary. The obtained values of the BSI index range from −1.9 to 0.7, while the average value is −0.9. To avoid negative values in the vegetation index (V) formula, a value of 1 has been added. Therefore, it reads:

$$V = 7.68 \times \ln(\text{BSI} + 1) + 8$$

2.4 Calculation of FFPI

The FFPI is created by gathering raster datasets of certain characteristics within the specified area and employing GIS technology to adjust, categorize, and merge the data. Figure 5 demonstrates the stages of data processing using the FFPI method. The outcome is a numerical gauge representing a region's susceptibility to flash flooding, which remains relatively consistent over time.

2.5 Verification of results using historical flood data

A field survey in Kratovo, North Macedonia, corroborated GIS and remote sensing findings by gathering firsthand data on flood events. Through interviews with residents and site visits, insights on flood frequency, impacts, and vulnerable areas were documented. This complemented the remote sensing analysis for a comprehensive flood risk assessment.

In order to validate the FFPI classification results, the methodology proposed by Yassin et al. [32] was followed, comparing the FFPI outcomes with historical flood data. This process is crucial for assessing the accuracy and reliability of the FFPI results. Historical flood data were obtained from field research and authoritative sources to ensure the credibility of the findings.

Landsat 8 satellite imagery was employed to observe flood events corresponding to historical data. The ENVI software, provided by Landsat, was utilized for processing and analyzing the imagery, including radiometric and atmospheric corrections to enhance quality [59]. ENVI's advanced tools for image classification, feature extraction, and change detection enabled accurate identification and delineation of flood-affected areas. This validation against historical data enhances the understanding of flash flood dynamics and aids in developing robust flood risk assessment and management strategies.

Additionally, WorldClim version 2 data [40] provided average precipitation data for 1970–2000 at a spatial resolution of 1 km. This high-resolution climate data, including total monthly precipitation and seasonality, was correlated with hotspot areas identified from historical flood observations. This correlation enhances flood risk assessment by providing detailed insights into precipitation patterns and their relationship with flood occurrences, aiding in targeted flood management strategies.

3 Results

3.1 Slope index

The slope map is interpolated from the 5-m Digital Elevation Model (DEM). Variation of the slope is one of the important factors affecting the timing of runoff and the amount of infiltration. The infiltration rate decreases with increasing slope angle [60]. The average slope value in the whole area is 21.1° (Table 3). The tributaries that are located in the eastern part of the Kratovska Reka catchment have a higher

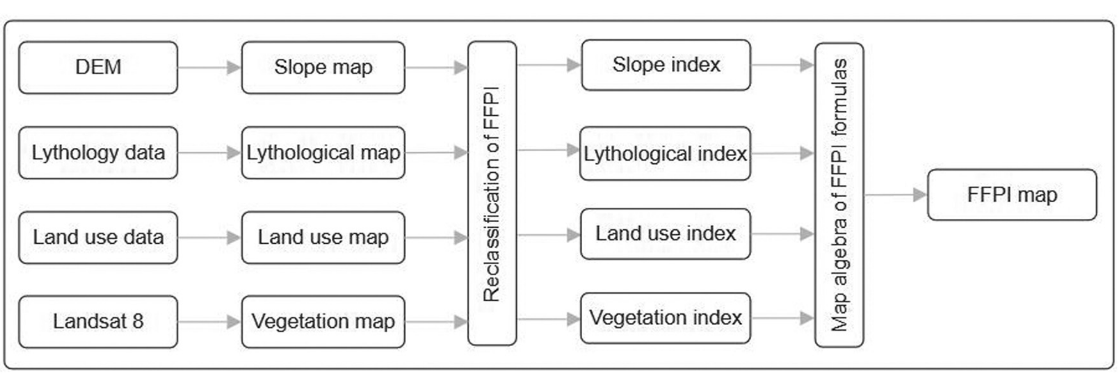

Figure 5: Flow chart with all the procedures and FFPI-based methodology used in this research.

Table 3: Average slope in degrees (s˚av)

Nu.	Sub-catchment	s˚av
1.	Lisečki Potok	23.5
2.	Nežilovski Potok	23.6
.3.	Drumski Potok	22.4
4.	Bela Reka	22.5
5.	Latišnica	24.6
6.	Tabački Dol	23.7
7.	Babakarina and Manceva Reka	23.4
8.	Mlački Dol	23.0
9.	Boškovačka Reka	19.9
10.	Raškovec	22.7
11.	Vrbički Dol	23.1
12.	Železnički Dol 1	22.7
13.	Železnički Dol 2	21.1
14.	Železnički Dol 3	16.2
15.	Šlegovski Dol	20.7
16.	Manev Dol	15.9
17.	Živalevski Dol	15.7
18.	Talašmanski Dol	15.2
19.	Topolovički Dol	15.3
20.	Ketenovski Dol	11.0
	Kratovska Reka	**21.0**

slope value, opposite to the tributaries that are managed in the western (lower) part of the catchment. Thus, the Sub-catchment of the river Latišnica has the highest average slope value (24.6°), and the Sub-catchment of Ketenovski Dol has the lowest average value (11°). The slope map in percent is calculated and classified. After this procedure, the model is classified into an FFPI value with the range from 1 to 10, and any slope of 30 degrees or higher is an FFPI of 10 (Figure 6).

3.2 Lithology index

In this study, the lithology index is generated from the lithological map [54], based on the five main lithological units, including clastic sediments, tuffs, solid volcanic (andesites), solid volcanic (dacitic ignimbrites), and schists. The classification of the lithological units was analyzed according to their susceptibility to torrential floods (Table 4).

The highest coefficient is assigned to river clastic sediments (9), which are most susceptible to flash floods, and the lowest to shale (3) with the least susceptibility to this geohazard. This index is very important because the percentage of these components in the units will affect infiltration rates and runoff during intense rainfall. Andesites and schists are less likely to contribute to flash floods

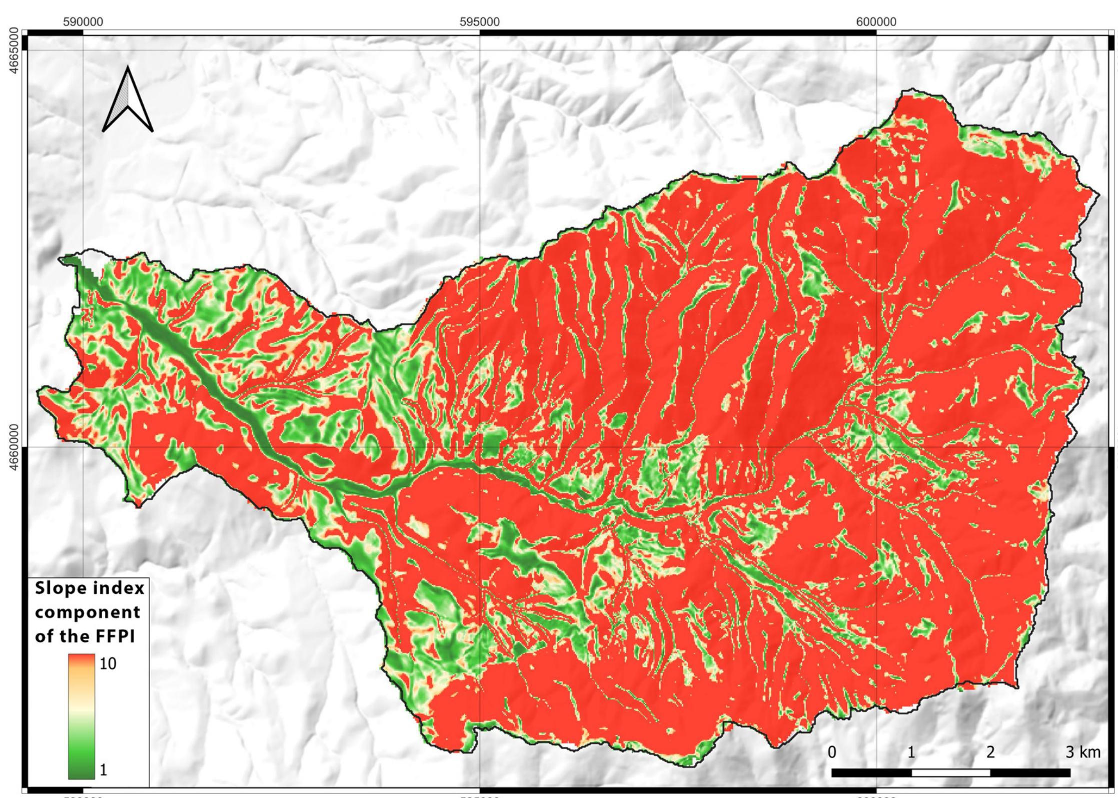

Figure 6: Slope index component of the FFPI for Kratovska Reka catchment.

Table 4: Coefficient of lithological units (*S*)

Lithological units	Geological period	Susceptibility to erosion processes	Coefficient, *S*
Clastic sediments	Pliocene	1	9
Tuffs	Pliocene	0.95	8
Solid volcanics (andesites)	Pliocene	0.2	5
Solid volcanics (dacitic ignimbrites)	Miocene	0.25	4
Schists	Riphean-Cambrian	0.8	3

because they are resistant to erosion. On the other hand, clastic sediments, tuffs, and dacitic ignimbrites are more susceptible to being eroded and transported during flash flood events, increasing the potential for flooding. The lithology index map is valued into an FFPI and illustrated in Figure 7.

Generally, the broadleaved forest and transitional forest shrubland are the two main types of land use structure. Based on the land use map, the land use index is generated and classified into the FFPI, and it is shown in Figure 8.

3.3 Land use index

The types of land use in the study area are shown in Table 5. Thus, the most susceptible terrains to FFPI are the non-irrigated agricultural surface, bare rocks, and areas with sparse vegetation, and the least susceptible are the areas under broad-leaved and mixed forests.

3.4 Vegetation index

The methodology described above provided thorough insights into the likelihood of flash floods and the intensity of erosion across the study area. By analyzing Landsat 8 satellite imagery and utilizing the Bare Soil Index (BSI), we were able to pinpoint areas at higher risk of flash

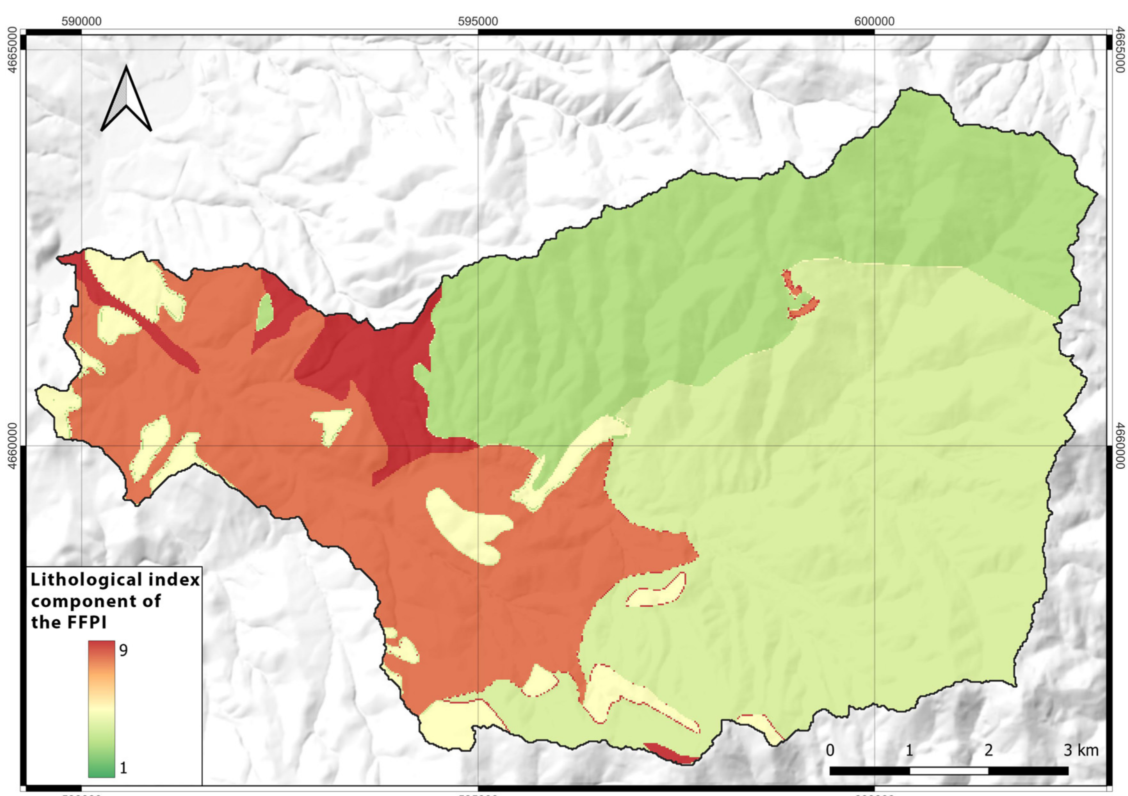

Figure 7: Lithology index component of the FFPI for Kratovska Reka catchment.

Table 5: Types of land use (*L*)

Classes of land	Value	Area (%)
Discontinuous urban environment	4	0.89
Non-irrigated farmland	9	0.06
Pastures	6	14.14
Complex land use	8	4.68
Agricultural land with significant areas under natural vegetation	7	13.51
Broadleaved forest	3	32.61
Mixed forest	3	1.17
Transitional forest shrubland	5	30.62
Bare rocks	9	1.33
Surfaces with sparse vegetation	9	1.01

floods with increased accuracy. Moreover, the correlation between vegetation density and erosion rate yielded valuable data for devising efficient land management strategies and implementing measures to mitigate the impact of flash flood events. The integration of remote sensing techniques and BSI computation significantly contributed to advancing our comprehension of erosion dynamics and the susceptibility of the study area to flash floods. The calculated value of the coefficient V ranges from 0 to 9.4, and the average is 3.7. A vegetation index is generated with a value from 1 to 9 (Figure 9).

3.5 FFPI

The GIS database has enabled the FFPI index to be run and to obtain information on the risk of flash floods for the catchment and sub-catchments (Table 6). According to the obtained calculations (Table 7), most of the catchment area belongs to the class with a medium probability of flash floods (72.04% or 49.34 km^2). High and very high flood susceptibility is 11.21% or 7.68 km^2. According to the model, the highest average coefficient of susceptibility to potential flash floods: Latišnica (2.16), Babakarina and Manceva Reka (2.11), Tabački Dol (2.06), Željeznički Dol 2 (2.03), and Dol Potok 1 (2.01). There is a low probability of flash floods, especially at the confluence of Kriva Reka (16.75% or 11.48 km^2). The average value of the Flash Potential Index (FFPI) is 1.9, considering that the values range from 1 to 5.

By processing and analyzing terrain slope, lithology, land types, land use, and BSI, a model of terrain susceptibility to flash floods was obtained (Figure 10).

3.6 Comparison of FFPI risk level with hotspot area of historical data of flash flood occurrence

In addition to GIS and remote sensing analysis, a field survey was conducted to validate the findings. The survey

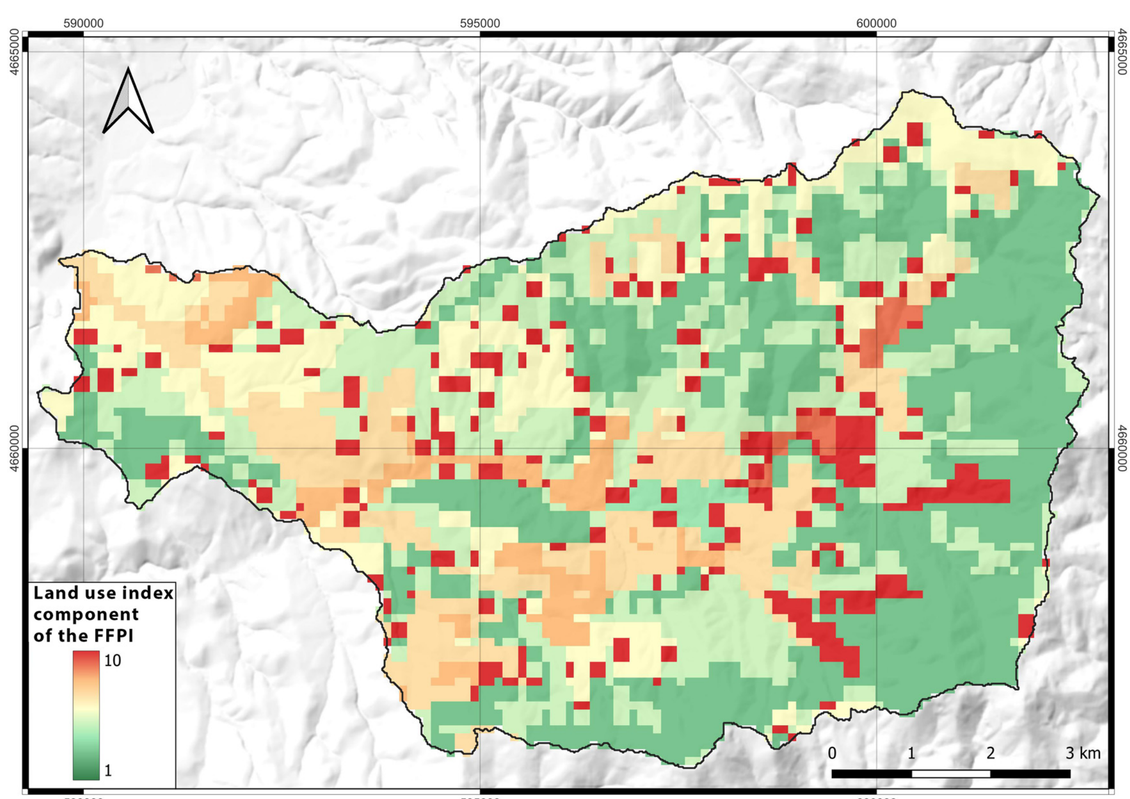

Figure 8: Land use index component of the FFPI for Kratovska Reka catchment.

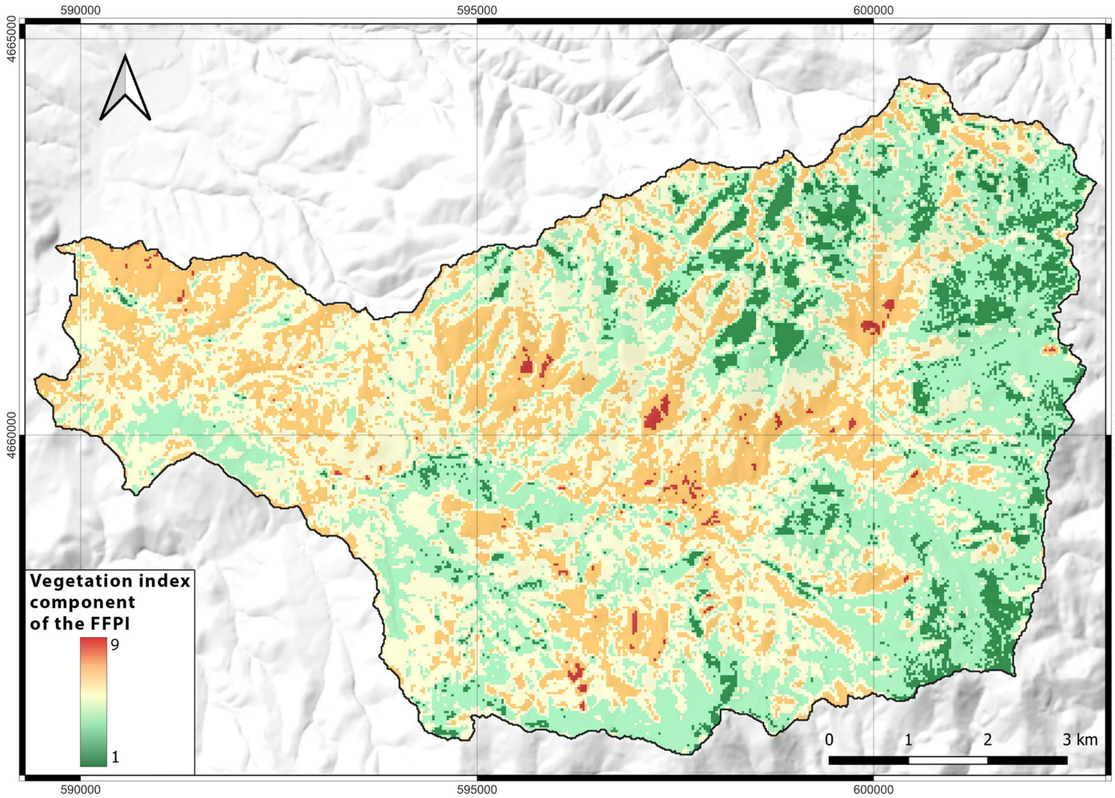

Figure 9: Vegetation index component of the FFPI for Kratovska Reka catchment.

Table 6: Potential flash flood index (FFPI) in the Kratovska Reka sub-catchments

Nu.	Sub-catchment	FFPI coefficient
1.	Lisečki Potok	1.98
2.	Nežilovski Potok	1.93
3.	Drumski Potok	1.85
4.	Bela Reka	1.93
5.	Latišnica	2.16
6.	Tabački Dol	2.06
7.	Babakarina and Manceva Reka	2.11
8.	Mlački Dol	1.91
9.	Boškovačka Reka	1.92
10.	Raškovec	1.96
11.	Vrbički Dol	1.93
12.	Železnički Dol 1	2.01
13.	Železnički Dol 2	2.03
14.	Železnički Dol 3	1.83
15.	Šlegovski Dol	1.97
16.	Manev Dol	1.82
17.	Živalevski Dol	1.96
18.	Talašmanski Dol	1.82
19.	Topolovički Dol	1.88
20.	Ketenovski Dol	1.52
	Kratovska Reka	**1.93**

focused on Kratovo town within the municipality of Kratovo, located in northeastern North Macedonia. It aimed to gather firsthand data on historical flood events through structured interviews with residents and site visits. Insights were obtained on flood frequency, duration, and local impacts. Key aspects included documenting past flood occurrences, identifying vulnerable areas and infrastructure, and capturing community perceptions on flood dynamics and resilience measures. This field data complemented the remote sensing analysis, providing crucial ground truth for validating the Landsat 8 imagery processed using ENVI software. Integrating field observations with

Table 7: Terrains susceptible to flash floods

Probability of flash flooding	Area	
	In km^2	In %
Weak	11.48	16.74
Moderate	49.34	71.95
High	6.48	9.45
Very high	1.28	1.87
Total	**68.58**	**100.00**

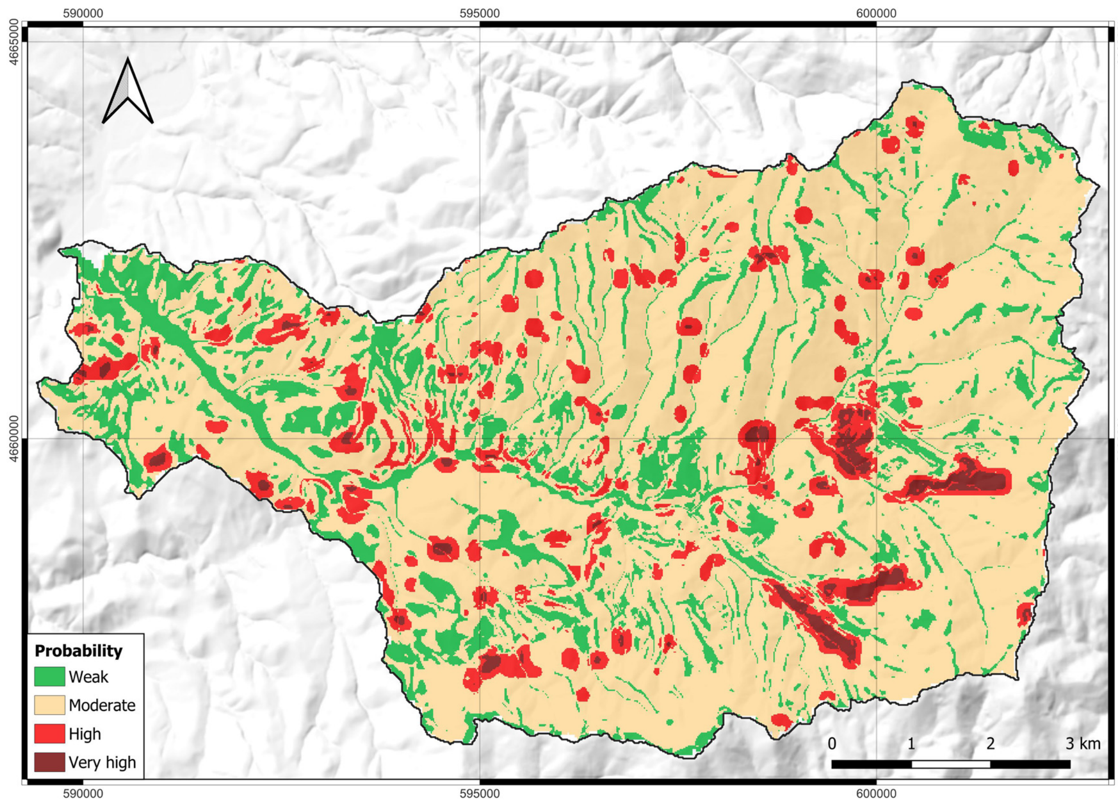

Figure 10: Susceptibility map to flash floods in the Kratovska Reka catchment.

remote sensing results enhances the comprehensiveness of flood risk assessment and management strategies tailored to the local context.

Thus, an examination of historical data has been undertaken to discern the areas prone to recurrent flash flood incidents within the specified time frame. The hotspot region for flash floods within the Kratovska Reka catchment is visually represented in Figure 11. Upon comparing with Figure 10, a notable observation emerges: the hotspot area for flash flood occurrences predominantly overlaps with the high-risk region susceptible to such events. It is noteworthy that this extreme-risk area has recorded numerous flooding events based on historical data analysis. This detailed comparison provides valuable insights into the distribution and severity of flash flood occurrences within the study area, thus informing future risk mitigation strategies and management efforts.

By combining GIS analysis, remote sensing techniques, and field surveys, we provided valuable insights into the factors influencing flash flood occurrences in the Kratovska Reka catchment area. This multi-faceted approach strengthens the credibility of the study findings and supports effective disaster preparedness and risk management strategies.

4 Discussion and concluding remarks

As mentioned earlier, it was observed that in an area identified as highly prone to flash flooding by FFPI, actual occurrences of flash floods were infrequent, which aligns with expectations based on the gathered data. This suggests that the findings from this section may not accurately represent the real situation, where extreme flash flooding is anticipated. This FFPI model incorporates additional variables such as Slope, Lithology, Land Use, and Vegetation Index. Previous studies have mainly focused on areas within river catchments where natural flash floods occur, which differs from the focus of this study. The study area is situated in a region where floods are predominantly caused by human activities, termed as urban flash floods. Infrastructure like drainage systems significantly influences urban flash floods. The absence of critical factors in this study may have impacted the outcomes. Precipitation is also vital to consider since prolonged and heavy rainfall typically triggers flash floods by elevating storm water levels.

Because of its intensity and spatial distribution, precipitation represents one of the most essential flash flood conditioning validation factors. Integration of WorldClim 2 precipitation data [40] with historical flood observations

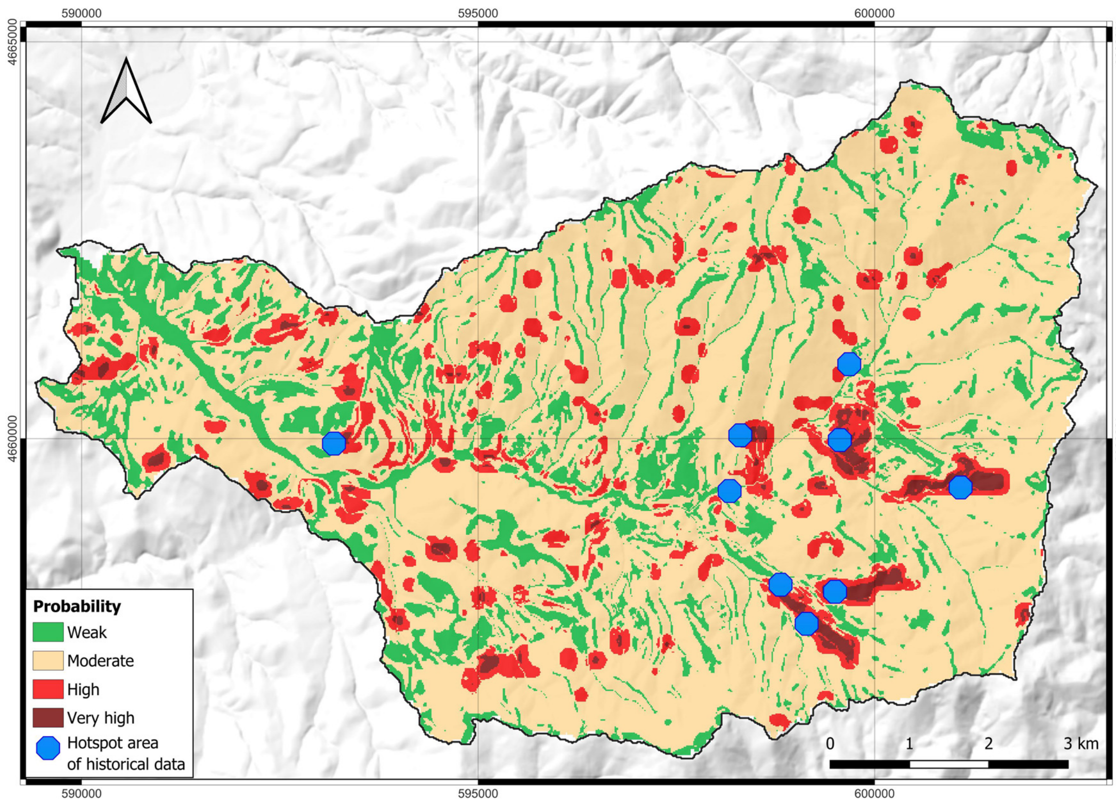

Figure 11: Hotspot Area based on historical data observations.

was conducted to enhance flood risk assessment. Thus, according to Aleksova et al. [7], intense and heavy rainfall often leads to the overflowing of the Kratovska Reka from its riverbed and the occurrence of flash floods. In summary, precipitation, especially heavy and intense precipitation, plays a central role in the validation of flash flood hotspot areas. The yearly precipitation in the catchment averages around 728.4 mm, peaking in May and November and dropping to a low in August. Approximately 57% of the annual precipitation occurs during the vegetation period, with spring and autumn receiving the most rainfall. Only about 9% of days see heavy rainfall exceeding 20.0 mm, with the possibility of reaching up to 110 mm per day. In winter, snow blankets the upper catchment, melting quickly in spring. To validate flash flood risks, intense rainfall data are crucial. However, lacking a pluviometry station in the area, we employed GIS Remote Sensing modeling and geospatial analysis. By overlaying average precipitation data with hotspot zones of historical data, we found that high-risk areas typically receive 700–750 mm of precipitation. The studies [38,61] on hazard areas in the catchment also validate this result. Although average rainfall alone isn't sufficient to forecast flash floods, it often coincides with areas experiencing lower average rainfall. This implies that regions with reduced rainfall typically have less vegetation and a slower recuperation from geohazards. Furthermore, factors such as geological composition, and historical deforestation over the past century increase erosion risks. The sub-catchment Latišnica (marked by a dashed line; Figure 12) has most of the hotspot areas in the whole catchment.

The FFPI is a model that provides an index ranging from 1 to 10, and given that the Kratovska Reka catchment's FFPI is at 49.34% for an index value of 5, which is the median, it can be classified as being at medium risk for flash floods. While the results are not entirely satisfactory, they do demonstrate the potential given that the primary factors have been considered. By incorporating an additional factor, such as the Stream Power Index (SPI), Topographic Wetness Index (TWI), Topographic Position Index (TPI), and Soil Index, more reasonable results may be obtained [32]. Furthermore, future research could integrate the Flood Vulnerability Index (FVI) Method to enhance the robustness of the analysis [62]. Given changes in both natural and human-influenced factors, it's advisable to establish a monitoring and control system to oversee ground conditions [63]. New technologies enable detailed surface data collection, which, when processed through GIS, can be used to create predictive

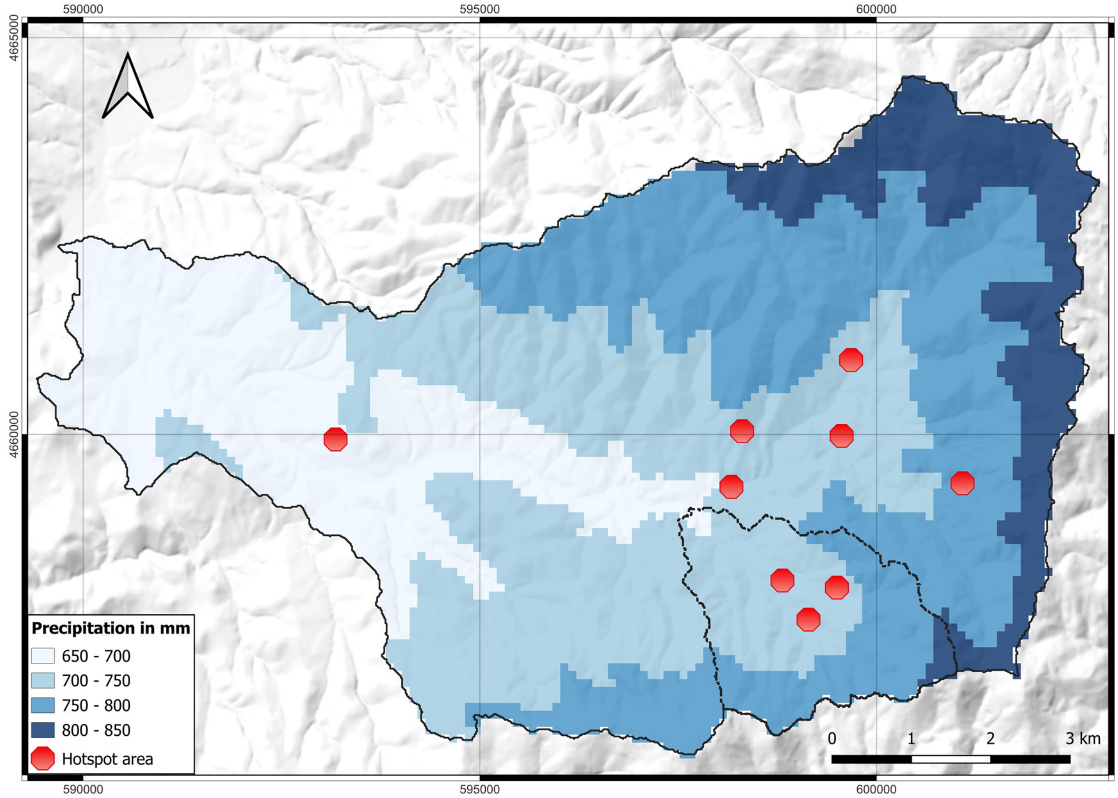

Figure 12: Integration of average precipitation data (WorldClim 2)[40] with hotspot areas based on historical data observations.

models. Such analysis is crucial for hazard prevention or mitigation, forming a vital part of spatial analysis [18]. However, the FFPI index overlooks factors like riverbed debris, landslides, and climate change impacts, necessitating comprehensive analyses with high-quality datasets and multiple methods to compare results. Despite each method having its pros and cons, employing various approaches can enhance effectiveness in assessing flash flood risks. It's essential to select the most suitable method for each situation to optimize solutions for the problem at hand.

Obtaining and analyzing the databases is straightforward, facilitated by both proprietary and open-source software accessible to spatial analysis professionals. The model introduced in this research could serve as a valuable approach for spatial planning endeavors, offering practical insights for land management and aiding local authorities in flash flood risk reduction efforts [34]. The methodology devised in this study is applicable across various contexts and can be implemented on a national scale within any river catchment. This is particularly relevant given the dynamic nature of land use and the rising occurrence of extreme weather events [22]. To mitigate the detrimental impacts of flash floods, it's crucial to identify and enact protective measures using a blend of GIS technology and on-site investigation. Collaborative efforts between local government bodies, alongside provincial and national services, can allocate resources for the deployment of biological and biotechnical interventions. These measures aim to substantially decrease the risk of severe torrential flooding in affected areas [10].

The combination of GIS and remote sensing has resulted in a potent tool for investigating and evaluating the potential for flash floods. The findings obtained through the FFPI method accurately reflect the risk of flash floods in the study area. This serves as a scientific foundation for managing natural resources at the local level [33]. Higher resolution historical data are needed for ROC curve analysis to quantitatively evaluate the flash flood model's accuracy. Standardizing and implementing other methodologies would enhance the monitoring and identification of natural hazards in North Macedonia on local and regional levels. This underscores the need for developing vulnerability assessments and management programs in southeastern Europe [24]. Also, understanding the barriers restraining the effective operation of flood early warning systems is crucial for improving disaster preparedness, minimizing loss of life and property, and enhancing community resilience to flood events [64].

For future research is relevant to incorporate machine learning methods to determine individual parameters' influence on flash flood occurrences more precisely [65]. These enhancements will enable more accurate susceptibility modeling, reducing subjectivity in assigning weighting factors and increasing the relevance of results for the specific regional area.

Acknowledgments: Slobodan B. Marković and Tin Lukić gratefully acknowledge the support of the Ministry of Science, Technological Development and Innovation of the Republic of Serbia (Grants No. 451-03-66/2024-03/200125 & 451-03-65/2024-03/200125) and the Provincial Secretariat for Higher Education and Scientific Research of Vojvodina (Serbia), No. 000871816 2024 09418 003 000 000 001 04 002 (GLOMERO), under Program 0201 and Program Activity 1012. The authors are grateful to the reviewers whose comments and suggestions greatly improved the manuscript.

Author contributions: Conceptualization, B.A.; methodology, B.A.; software, B.A.; validation, B.A., T.L., and I.M.; formal analysis, B.A.; investigation, B.A.; resources, B.A., I.M., and T.L.; data curation, B.A., T.L., and I.M.; writing – original draft preparation, B.A. and T.L.; writing – review and editing, B.A., I.M., R.M., S.B.M., V.M.C., T.L.; visualization, B.A.; supervision, I.M., R.M., and T.L.; project administration, B.A.; funding acquisition, T.L. All authors have read and agreed to the published version of the manuscript.

Conflict of interest: The authors state no conflict of interest.

References

[1] Blešić I, Ivkov M, Tepavčević J, Popov Raljić J, Petrović MD, Gajić T, et al. Risky travel? Subjective vs. Objective perceived risks in travel behaviour—Influence of hydro-meteorological hazards in South-Eastern Europe on Serbian tourists. Atmosphere. 2022;13:1671. doi: 10.3390/atmos13101671.

[2] Lukić T, Gavrilov MB, Marković SB, Komac B, Zorn M, Mladjan D, et al. Classification of the natural disasters between the legislation and application: Experience of the Republic of Serbia. Acta Geogr Slov. 2013;53:149–64.

[3] Lukić T, Lukić A, Basarin B, Ponjiger TM, Blagojević D, Mesaroš M, et al. Rainfall erosivity and extreme precipitation in the Pannonian basin. Open Geosci. 2019;11:664–81.

[4] Blöschl G, Hall J, Viglione A, Perdigão RAP, Parajka J, Merz B, et al. Changing climate both increases and decreases European river floods. Nature. 2019;573:108–11. doi: 10.1038/s41586-019-1495-6.

[5] Turconi L, Faccini F, Marchese A, Paliaga G, Casazza M, Vojinovic Z, et al. Implementation of nature-based solutions for hydro-meteorological risk reduction in small mediterranean catchments: The Case of Portofino Natural Regional Park, Italy. Sustainability. 2020;12:1240.

[6] Micić Ponjiger T, Lukić T, Basarin B, Jokić M, Wilby RL, Pavić D, et al. Detailed analysis of spatial–temporal variability of rainfall erosivity and erosivity density in the Central and Southern Pannonian basin. Sustainability. 2021;13:13355. doi: 10.3390/su132313355.

[7] Aleksova B, Lukić T, Milevski I, Puhar D, Marković SB. Preliminary assessment of geohazards' impacts on geodiversity in the Kratovska Reka catchment (North Macedonia). Geosciences. 2024;14:62. doi: 10.3390/geosciences14030062.

[8] Micić Ponjiger T, Lukić T, Wilby RL, Marković SB, Valjarević A, Dragićević S, et al. Evaluation of rainfall erosivity in the Western Balkans by mapping and clustering ERA5 reanalysis data. Atmosphere. 2023;14:104. doi: 10.3390/atmos14010104.

[9] Trobec T. Spatio-temporal distribution of flash floods in Slovenia. Dela. 2016;46:5–20.

[10] Durlević U, Novković I, Lukić T, Valjarević A, Samardžić I, Krstić F, et al. Multi-hazard susceptibility assessment: A case study – Municipality of Štrpce (Southern Serbia). Open Geosci. 2021;13(1):1414–31. doi: 10.1515/geo-2020-0314.

[11] Dragićević S, Kostadinov S, Novković I, Momirović N, Langović M, Stefanović T, et al. Assessment of soil erosion and torrential flood susceptibility: Case study—Timok River Basin, Serbia. In book: The lower Danube river, hydro-environmental issues and sustainability. Cham: Springer; 2022. doi: 10.1007/978-3-031-03865-5_12.

[12] Lazarević K, Todosijević M, Vulević T, Polovina S, Momirović N, Caković M. Determination of flash flood hazard areas in the Likodra watershed. Water. 2023;15(15):2698. doi: 10.3390/w15152698.

[13] Krvavica N, Šiljeg A, Horvat B, Panđa L. Pluvial flash flood hazard and risk mapping in Croatia: Case study in the Gospić catchment. Sustainability. 2023;15(2):1197. doi: 10.3390/su15021197.

[14] Marchi L, Borga M, Preciso E, Gaume E. Characterization of selected extreme flash floods in Europe and implications for flood risk management. J Hydrol. 2010;394(1–2):118–33.

[15] Dragićević S, Filipović D. Natural conditions and disasters in planning to protect space. 2nd edn. Belgrade: University of Belgrade - Geography faculty (In Serbian); 2016.

[16] Gavrilović LJ. Floods in SR Serbia in the 20th century - causes and consequenc. es. Special issue SGD, no. 52. Belgrade: Serbian geographical society (In Serbian); 1981.

[17] Petrović A. Flash floods in Serbia. Special editions SGD, book 73. Belgrade: Serbian Geographical Society (In Serbian); 2021. ISBN 978-86-82751-62-5.

[18] Jovanović D. Application of the flash flood potential index in torrential floods risk assessment (FFPI): A case study of Svilajnac municipality. Proc - Faculty Geogr, Univ Belgrade. 2023;(71):65–78. doi: 10.5937/zrgfub2371065J.

[19] Kourgialas NN, Karatzas GP. Flood management and a GIS modeling method to assess flood-hazard areas—a case study. Hydrol Sci J. 2011;56:212–25.

[20] Shawaqfah M, Almomani F, Khatatbeh AA. Mapping flash flood potential and risk level using GIS techniques and the flash flood potential index (FFPI) in Amman Zarqa Basin of Jordan. Jordanian J Eng Chem Ind. 2020;3(3):81–90. doi: 10.48103/jjeci3102020.

[21] Chen C, Peihua X, Yihong W, Jianping C, Lianjing Z, Cencen N. Flash flood hazard susceptibility mapping using frequency ratio and statistical index methods in coalmine subsidence areas. Sustainability, MDPI. September 2016;8:1–18.

[22] Cristian PM, Simion A, Peptenatu D, Dima C, Draghici C, Florescu MS, et al. Spatial assessment of flash-flood vulnerability in the Moldova river catchment (N Romania) using the FFPI. J Flood Risk Manag. 2020;13(1). doi: 10.1111/jfr3.12624.
[23] Kruzdlo R, Ceru J Flash Flood Potential Index for WFO Mount Holly/ Philadelphia. http://bgmresearch.eas.cornell.edu/research/ ERFFW/posters/kruzdlo_ FlashFloodPotentialIndexforMountHollyHSA.pdf (accessed on 02.03.2024)
[24] Aleksova B, Milevski I, Dragićević S, Lukić T. GIS-based integrated multi-hazard vulnerability assessment in Makedonska Kamenica Municipality, North Macedonia. Atmosphere. 2024;15:774. doi: 10. 3390/atmos15070774.
[25] Lincoln S, Zogg J, Brewster J Addition of a Vulnerability Component to the Flash Flood Potential Index. 2016; Available: https://www. weather.gov/media/lmrfc/tech/2016_Vulnerability_Component_ FFPI.pdf.
[26] Arachchige D. Mapping flash flood potential using GIS and the Flash Flood Potential Index (FFPI) in the Turtle River and Forest River watersheds in North Dakota. Dissertation. The University of North Dakota; 2015.
[27] Teodor S, Matreata S. A way of determining how small river basins of Some's River are susceptible to flash floods. Carpath J Earth Env. 2011;6:89–98.
[28] Zaharia L, Costache R, Pravalie R, Minea G. Assessment and mapping of flood potential in the Slanic catchment in Romania. J Earth Syst Sci. 2015;124:1311–24.
[29] Minea G. Assessment of the flash flood potential of Bâsca river catchment (Romania) based on physiographic factors. Cent Eur J Geosci. 2013;5(3):344–53.
[30] Pravalie R, Costache R. The analysis of the susceptibility of the flash-floods' genesis in the area of the hydrographical basin of Basca Chiojdului river. Forum Geogr. 2014;13:39–49.
[31] Karagiorgos K, Thaler T, Heiser M, Hubl J, Fuchs S. Multi-vulnerability analysis for flash flood risk management. Nat Hazards. 2016;82:63–87.
[32] Yassin NA, Nor Adnan NA, Sadek EM. Analysis of flash flood potential index (FFPI) and scenarios assessment in Shah Alam using GIS approach. Plan Malays. 2023;21:1–12. doi: 10.21837/pm. v21i26.1255.
[33] Popescu N-C, Bărbulescu A. Flood hazard evaluation using a flood potential index. Water. 2023;15(20):3533. doi: 10.3390/ w15203533.
[34] Kocsis I, Stefan B, Ioan-Aurel I, Dohotar V, Rusu R, Rosca S. Flash flood vulnerability mapping based on FFPI using GIS spatial analysis case study: Valea Rea catchment area, Romania. Sensors. 2022;22(9):3573. doi: 10.3390/s22093573.
[35] Milevski I. Natural hazards in the Republic of Macedonia with special emphasis on flood and earthquake in Skopje. Geogr Rev. 2017;50(5–22):2016.
[36] Milevski I, Dragićević S, Zorn M. Statistical and expert-based landslide susceptibility modeling on a national scale applied to North Macedonia. Open Geosci. 2019;11(1):750–64. doi: 10.1515/geo-2019-0059.
[37] Milevski I, Dragićević S, Radevski I. GIS and remote sensing based natural hazard modeling of Kriva River catchment, Republic of Macedonia. Z für Geomorphol Suppl Iss. 2017;61(2):213–28.
[38] Aleksova B, Lukić T, Milevski I, Spalević V, Marković SB. Modeling water erosion and mass movements (Wet) by using GIS-based multi-hazard susceptibility assessment approaches: A Case Study—Kratovska Reka catchment (North Macedonia). Atmosphere. 2023;14:1139. doi: 10.3390/atmos14071139.
[39] Milevski I. An approach of GIS-based assessment of soil erosion rate on country level in the case of Macedonia. In Proceedings of the Conference Geobalcanica, Skopje, North Macedonia, 5–7 June. Vol. 1, 2015.
[40] Fick SE, Hijmans RJ. Worldclim 2: New 1-km spatial resolution climate surfaces for global land areas. Int J Climatol. 2017;37(12):4302–15.
[41] Costache R, Pravalie R, Mitof I, Popescu C. Flood vulnerability assessment in the low sector of Saratel catchment. Case study: Joseni village. Carpathian J Earth Env Sci. 2015;10(1):161–9.
[42] Tincu R, Lazar G, Lazar I. Modified flash flood potential index in order to estimate areas with predisposition to water accumulation. Open Geosci. 2018;10:593–606.
[43] Marković R, Mudelsee M, Radaković MG, Radivojević AR, Schaetzl RJ, Basarin B, et al. An index for snowmelt-induced landslide prediction for Zavoj Lake, Serbia. Atmosphere. 2024;15(3):256. doi: 10.3390/atmos15030256.
[44] Petrović A, Kostadinov S, Dragićević S. The inventory and characterization of torrential flood phenomenon in Serbia. Pol J Environ Stud. 2014;23(3):823–30.
[45] Petrović A, Dragićević S, Radić B, Milanović Pešić A. Historical torrential flood events in the Kolubara river basin. Nat Hazards. 2015;79:537–47. doi: 10.1007/s11069-015-1860-1.
[46] Smith G Flash Flood Potential: Determining the Hydrologic Response of FFMP Basins to Heavy Rain by Analyzing Their Physiographic Characteristics. 2003; Available at https://www. cbrfc.noaa.gov/papers/ffp_wpap.pdf.
[47] Smith G. Development of a flash flood potential index using physiographic data sets within a geographic information system. MS thesis. University of Utah; 2010.
[48] Ristić R, Radić B, Vasiljević N. Characteristics of maximal discharges on torrential watersheds in Serbia. Bull Serbian Geogr Soc. 2009;89(4):161–89.
[49] Minea G, Iliescu M, Dedu F. Temporal rainfall properties at events scale in the Curvature Subcarpathians (Romania). Forum Geografic. 2016;15:115–23.
[50] Kostadinov S, Dragićević S, Stefanović T, et al. Torrential flood prevention in the Kolubara river basin. J Mounain Sci. 2017;14(11):2230–45. doi: 10.1007/s11629-017-4575-9.
[51] Saleh A, Yuzir A, Abustan I. Flash flood susceptibility modelling: A review. IOP Conf Ser: Mater Sci Eng. 2020;712:012005.
[52] Band SS, Janizadeh S, Chandra Pal S, Saha A, Chakrabortty R, Melesse AM, et al. Flash flood susceptibility modeling using new approaches of hybrid and ensemble tree-based machine learning algorithms. Remote Sens. 2020;12:3568. doi: 10.3390/ rs12213568.
[53] Islam A, Talukdar S, Mahato S, Kundu S, Eibek KU, Pham QB, et al. Flood susceptibility modelling using advanced ensemble machine learning models. Geosci Front. May 2021;12(3):101075.
[54] Basic geological map of SFRY, Kratovo sheet, 100k. Federal Geological Institute Belgrade, 1974.
[55] Copernicus. Corine Land Cover 2018: Copernicus Land Monitoring Service; Technical Report; Office for Official Publications of the European Communities: Luxembourg, 2016.
[56] United States Geological Survey. Landsat 8 program taken by Earth Explorer. United States Geological Survey (accessed on Feb 20, 2024).

[57] Kumar N, Singh SK. Soil erosion assessment using earth observation data in a trans-boundary river basin. Nat Haz. 2021;107:1–34.

[58] Diek S, Fornallaz F, Schaepman M, De Jong R. Barest pixel composite for agricultural areas using Landsat time series. Remote Sens. 2017;9:1245.

[59] Chen X, Liu D, Gao Y. Monitoring of urban flood inundation dynamics using Landsat time-series images and Google Earth Engine. Remote Sens. 2019;11(2):160.

[60] Fox D, Bryan RB, Price AG. The influence of slope gradient on infiltration rate for interrill conditions. Geoderma. 1997;80(1-2):181–94. doi: 10.1016/S0016-7061(97)00075-X.

[61] Aleksova B. Correlation of geodiversity and geohazards in the Kratovska Reka catchment (North Macedonia). Master thesis. Skopje, North Macedonia: Faculty of Natural Sciences and Mathematics, Ss Cyril and Methodius University; University Bulletin (In Macedonian); 2024.

[62] Aktar MA, Shohani K, Hasan MN, Hasan MK. Flood vulnerability assessment by flood vulnerability index (FVI) method: A study on Sirajganj Sadar Upazila. Int J Disaster Risk Manag. 2021;3(1):1–14. doi: 10.18485/ijdrm.2021.3.1.1

[63] Vujačić D, Milevski I, Mijanović D, Vujović F, Lukić T. Initial results of comparative assessment of soil erosion intensity using the WIntErO model: A case study of Polimlje and Shirindareh drainage basins. Carpath J Earth Env Sci. 2023;18:385–404. doi: 10.26471/cjees/2023/018/267.

[64] Sukhwani V, Gyamfi BA, Zhang R, AlHinai AM, Shaw R. Understanding the barriers restraining effective operation of flood early warning systems. Int J Disaster Risk Manag. 2019;1(2):1–19. doi: 10.18485/ijdrm.2019.1.2.1.

[65] Šiljeg S, Milošević R, Mamut M. Pluvial flood susceptibility in the local community of the City of Gospić (Croatia). Sustainability. 2024;16:1701. doi: 10.3390/su16041701.